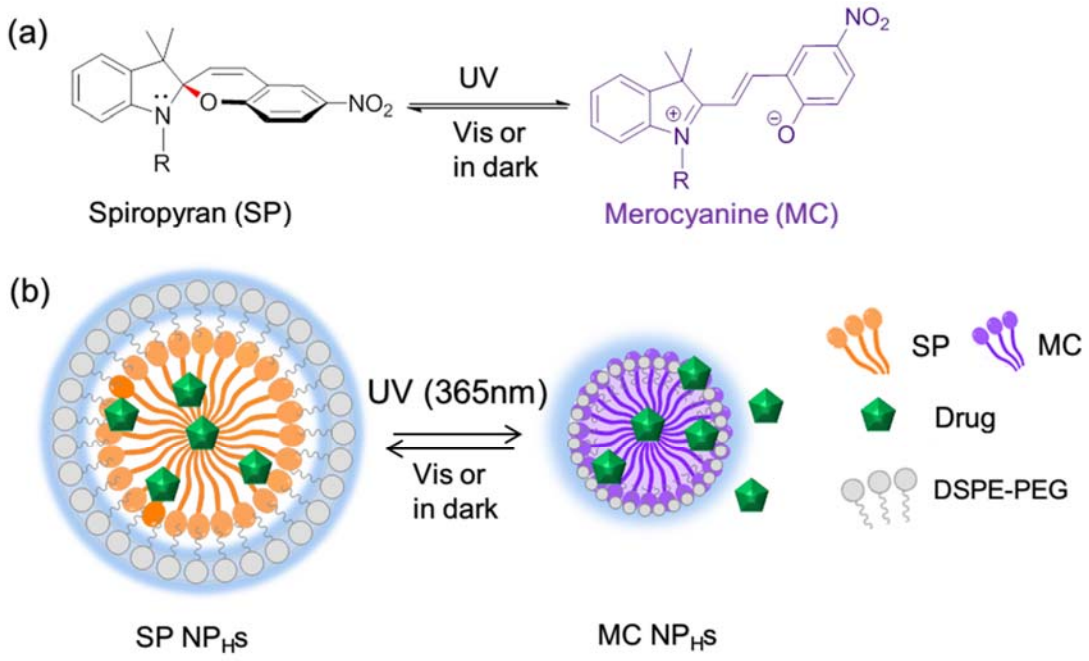

Figure S1. Scheme of the photoswitching of spiropyran and its nanoparticulate formulation. (a) Structure and photo-isomerization reaction between spiropyran (SP) and merocyanine (MC). (b) Scheme of photo-switchable SP / DSPE-PEG lipid hybrid nanoparticles (NP_{HS}).

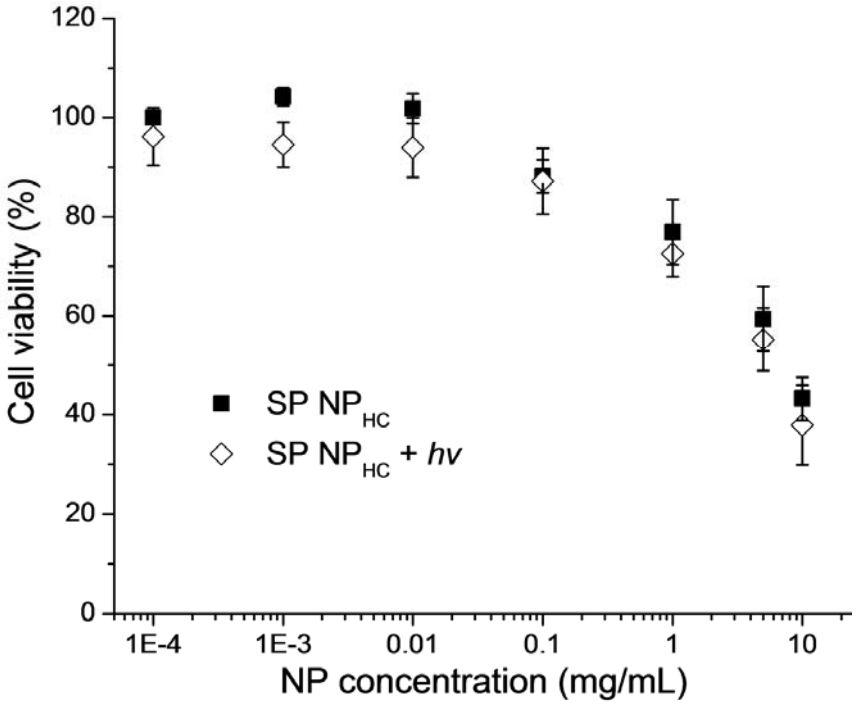

Figure S2. Effect of SP NP_{HC}s on viability of HT-1080 cells. Cells were incubated with SP NP_{HC}s at various concentrations for 4 hours, washed with NP-free media, then irradiated with UV irradiation (365 nm, 10s, 1W/cm^2) or not. Cells were further incubated for a total time of 24 h at 37^{o}C before the assaying viability by MTT assay. Data are means ± SD, N=6. SP NP_{HC}s: spiropyran hybrid nanoparticles containing cholesterol.

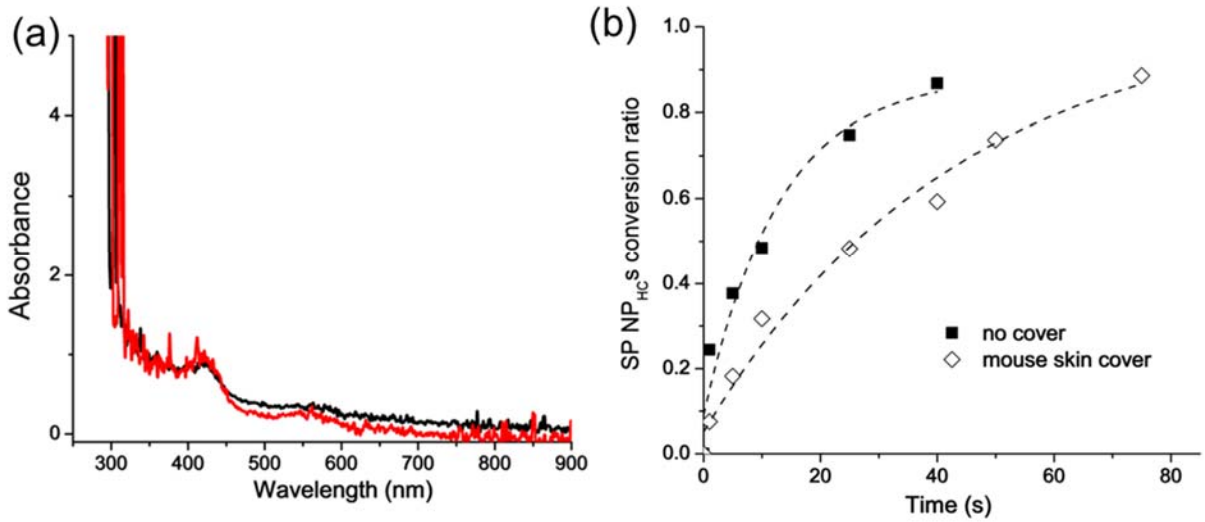

Figure S3. Ex vivo photo-switching of SP NP_{HC} through mouse skin. (a) Absorbance spectra of mouse skin. Red line: skin from *nu/nu* nude mice bearing HT-1080 tumors; black line: skin from *nu/nu* mice without tumor inoculation. (b) Conversion over time of SP NP_{HC}s to MC NP_{HC}s upon UV irradiation at 365 nm at 1W/cm^2, with or without intervening mouse skin.

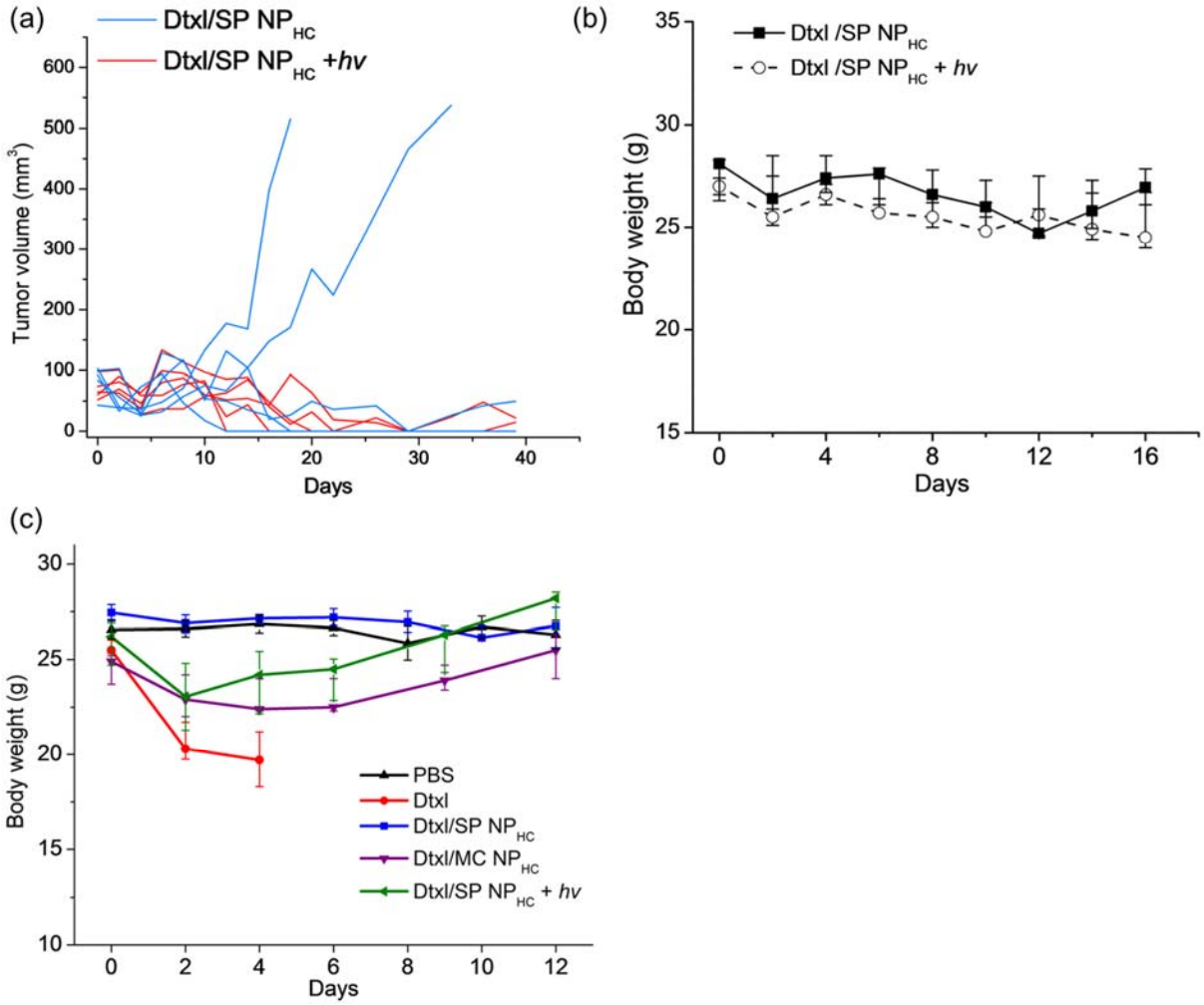

Figure S4. Tumor volume and mouse body weight changes after intratumoral (see Figure 2d) or intravenous treatments (see Figure 3a). (a) Tumor volume in individual animals after intratumoral injection of Dtxl/SP NP_{HC} (blue line) or same particles with light irradiation (black line), which was described in Figure 2d. (b-c) Mouse body weight during the tumor growth inhibition study described in (b) Figure 2 (intratumoral injection, N=5), and (c) Figure 3 (intravenous injection, N=5). In (c), severe body weight loss was observed within 4 days in the group treated with free Dtxl (red line). Data are medians ± quartiles. Dtxl: docetaxel.

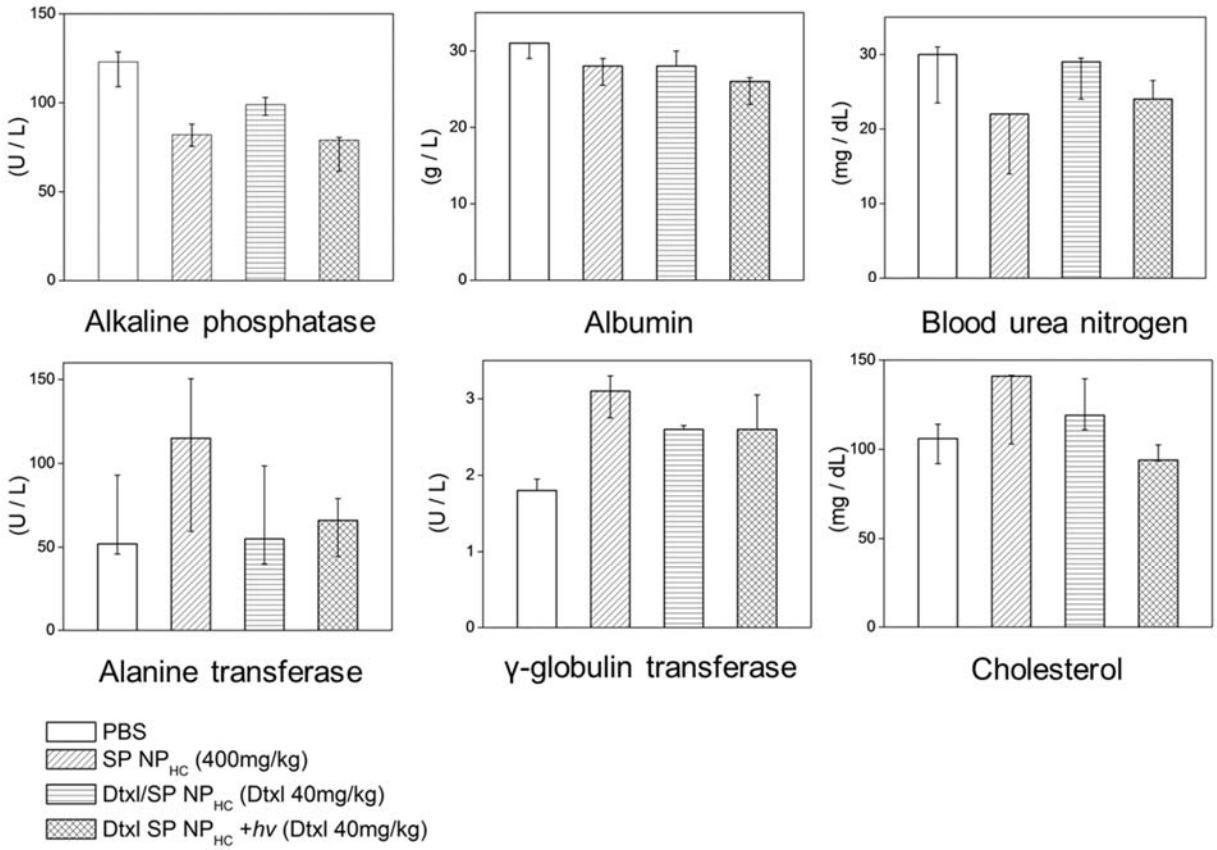

Figure S5. Liver function parameters in mice 14 days after intravenous injection of various formulation (N=4). Data are medians ± quartiles.

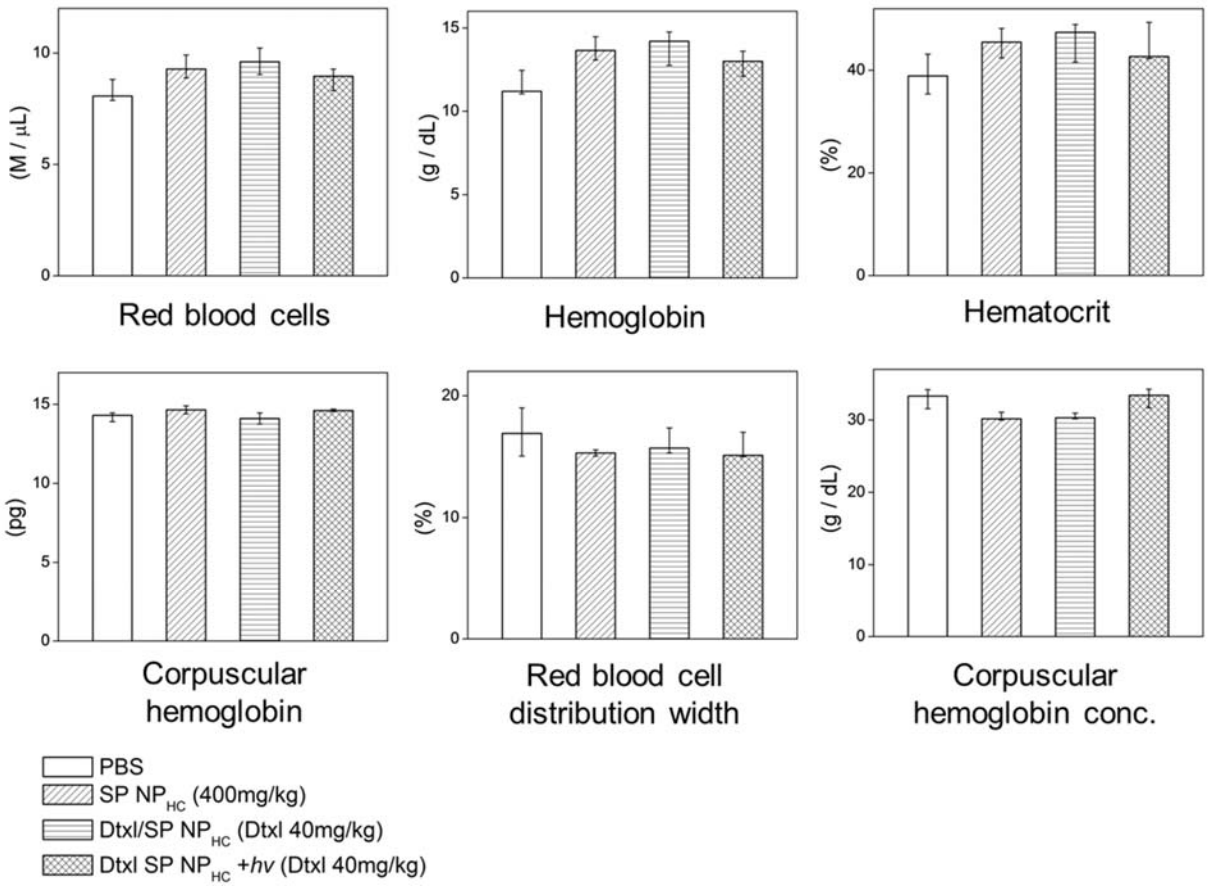

Figure S6. Erythrocytes parameters in mice 14 days after intravenous injection of various formulation (N=4). Data are medians ± quartiles.

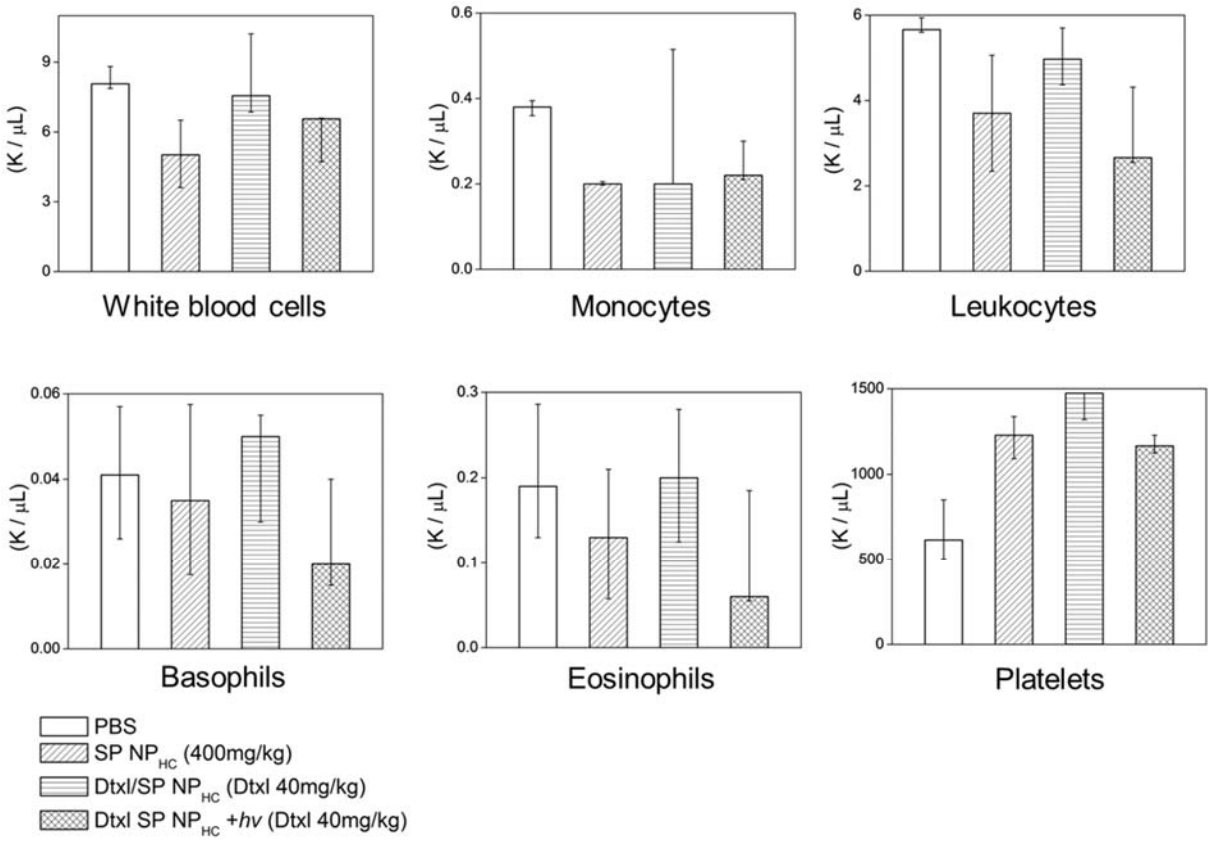

Figure S7. Leukocyte and platelet counts in mice 14 days after intravenous injection of various formulations (N=4). Data are medians ± quartiles.

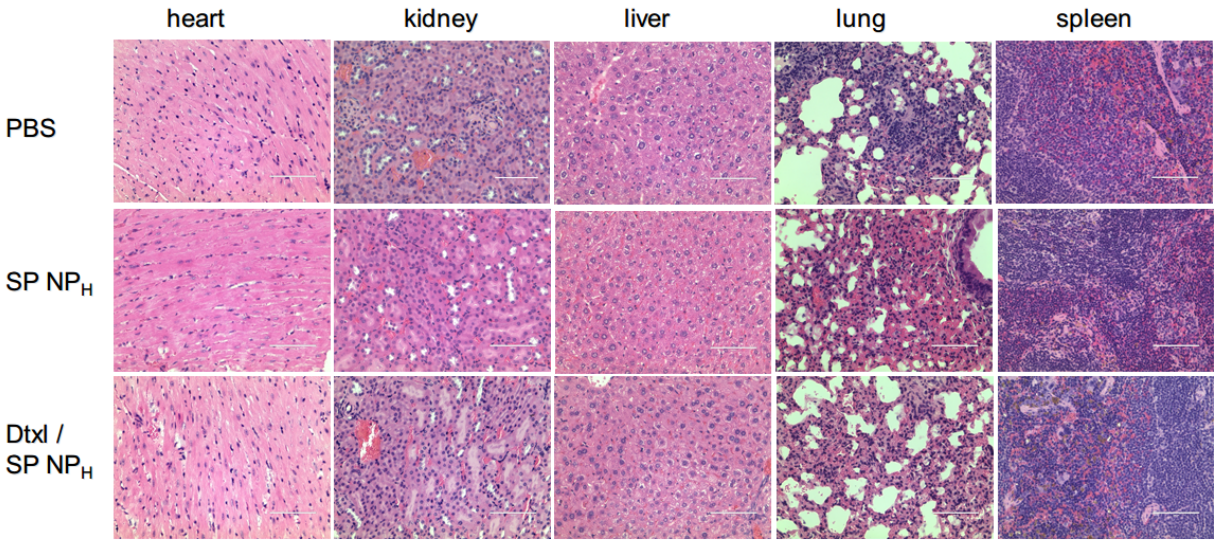

Figure S8. Histological images of organs from animals receiving different treatments. Hemotoxylin and eosin stained sections of tissues of mice treated with PBS, SP NP_{HC} (400 mg/kg) or Dtxl / SP NP_{HC} (40mg/kg) 72 hours after i.v. injection.

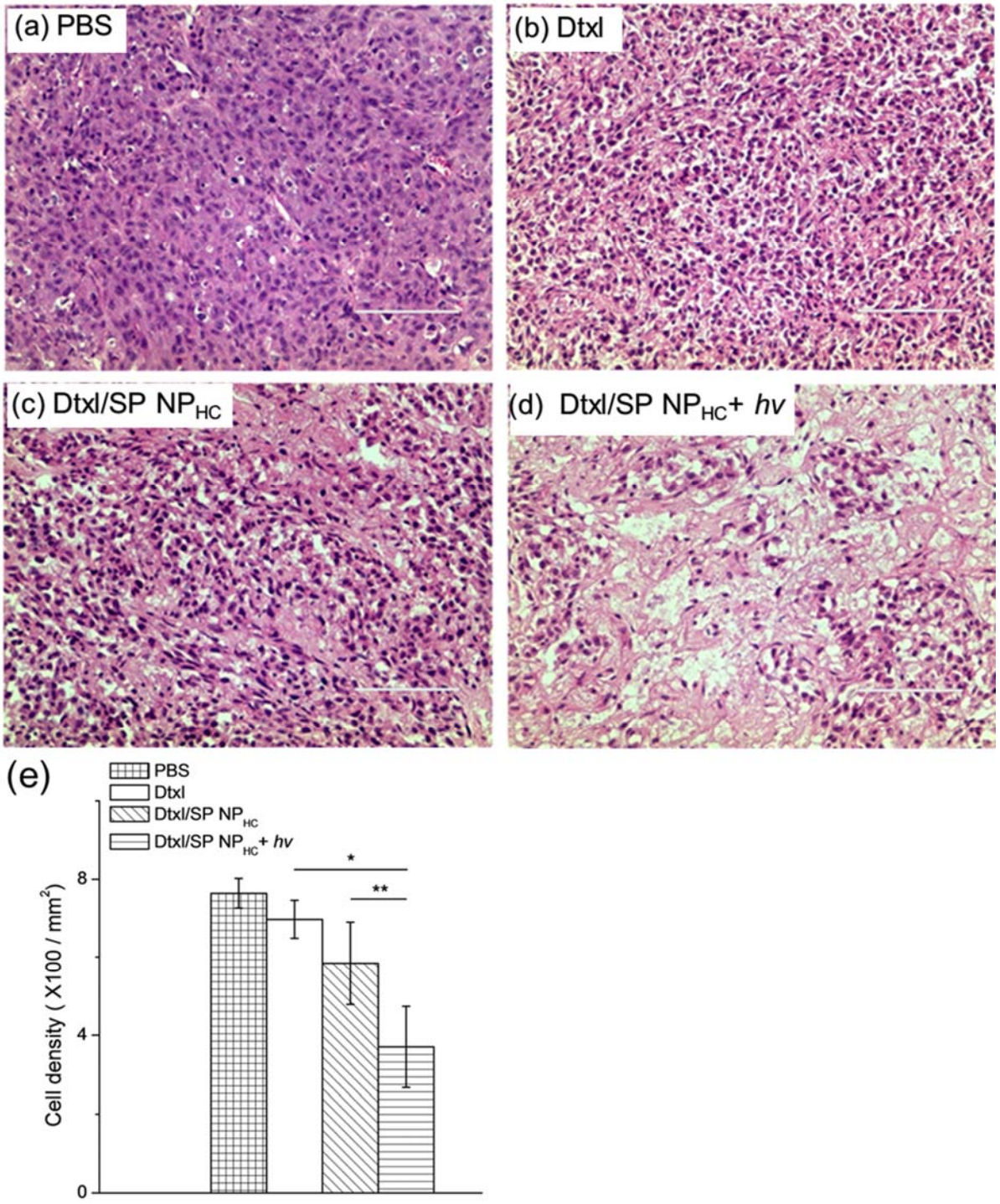

Figure S9. Histological analysis of HT-1080 tumor tissues following different treatments. (a-d) Representative hematoxylin and eosin stained sections of tumor tissues collected from animals 96 h after intravenous injection of (a) PBS; (b) free Dtxl (10 mg/kg); (c) Dtxl/SP NP_{HC}s (40 mg/kg) and (d) Dtxl/SP NP_{HC}s+*hv* (40 mg/kg). Scale bar: 100 μm. (e) Tumor cell density counts of (a-d). Dtxl/SP NP_{HC}s with light triggering significantly reduced tumor cells after 96 hours. **P*<0.005; ***P*=0.029.

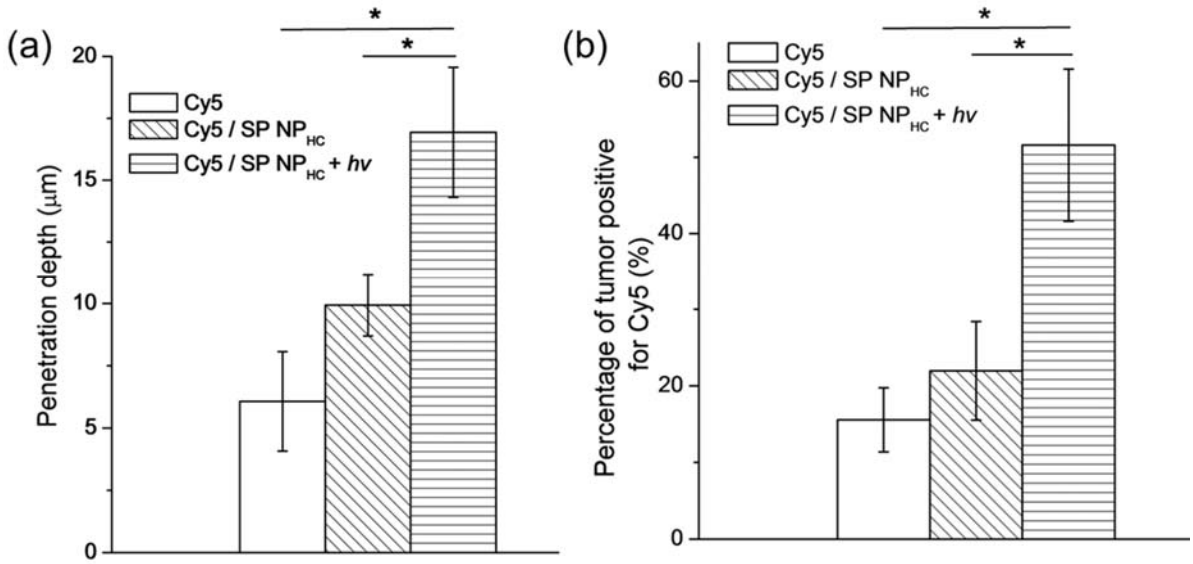

Figure S10. Effect of light triggering on intratumoral penetration of Cy5/SP NP_{HC}. Quantification of (a) nanoparticle penetration depth, i.e. the distance from the blood vessels where the fluorescence intensity of extravasated Cy5 or Cy5/SP NP_{HC}s fell to half-maximal (Methods S9), and (b) the fraction of tumor area positive for Cy5. (For all data, N=16 sections, with 4 sections per tumor from 4 tumors.) All data are means ± SD. *P<0.001

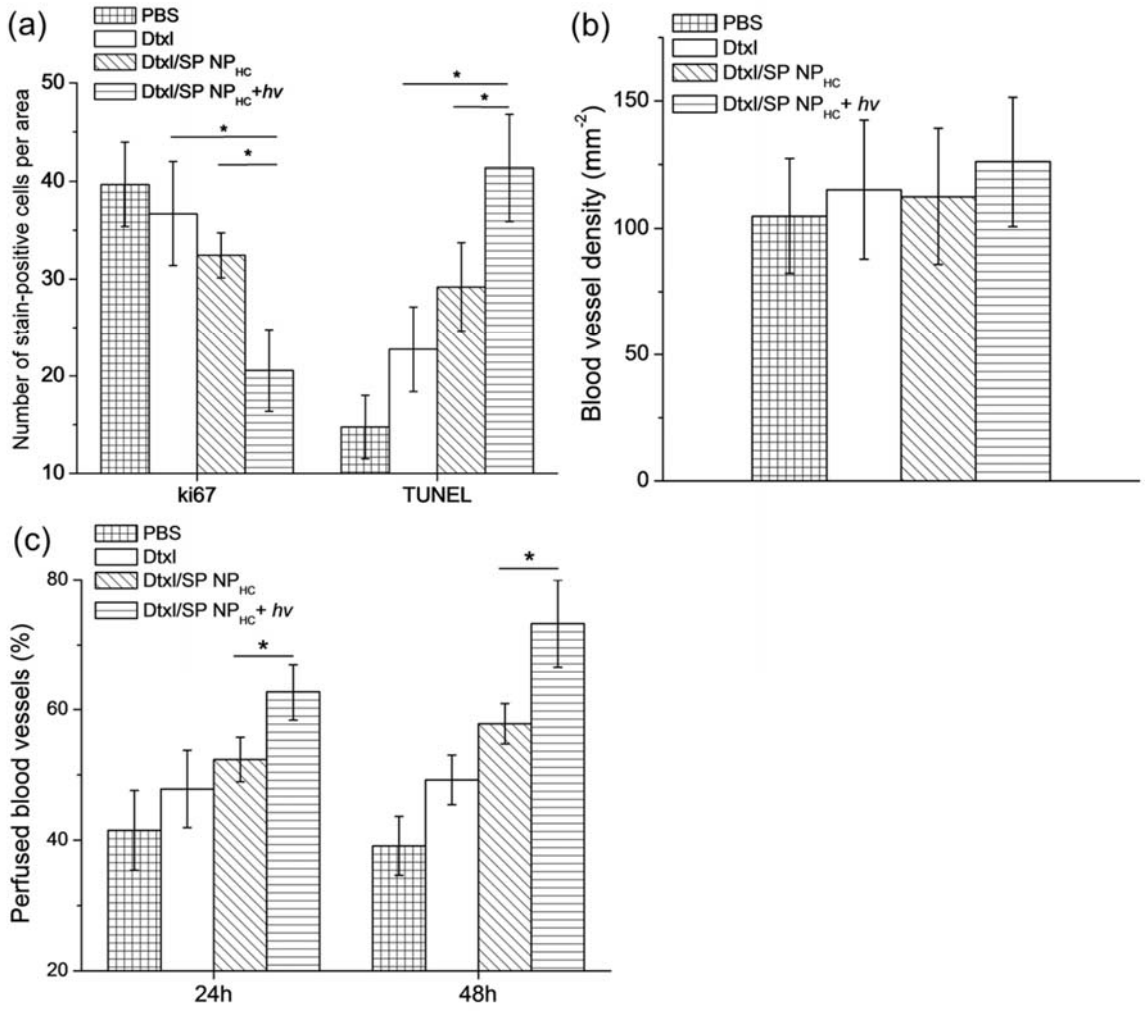

Figure S11. Effect of light-triggering on Dtxl/SP NP_{HC}-induced tumor cell apoptosis, tumor blood vessel perfusion, and blood vessel density. (a) Effect of light-triggering of Dtxl/SP NP_{HC} (Dtxl 40mg/kg) on tumor cell proliferation (ki67 positive) and apoptosis (TUNEL positive) at 24 h after injection (N=4, with 4 sections per tumor and 4 tumors per group; * indicates $P<0.01$). Data are the number of stain-positive cells per 0.04 mm^2 area (for $ki67^+$, 200μm×200μm), or per 0.36 mm^2 (for TUNEL, 600μm×600μm). (b) Blood vessel density was similar between groups (P not significant, N=4). (c) Effect of treatment group on blood vessel perfusion, quantified by comparing perfused vessels (FITC-lectin) with total blood vessels stained by anti-CD31. (N=4, with* $P<0.01$) All data are means ± SD.

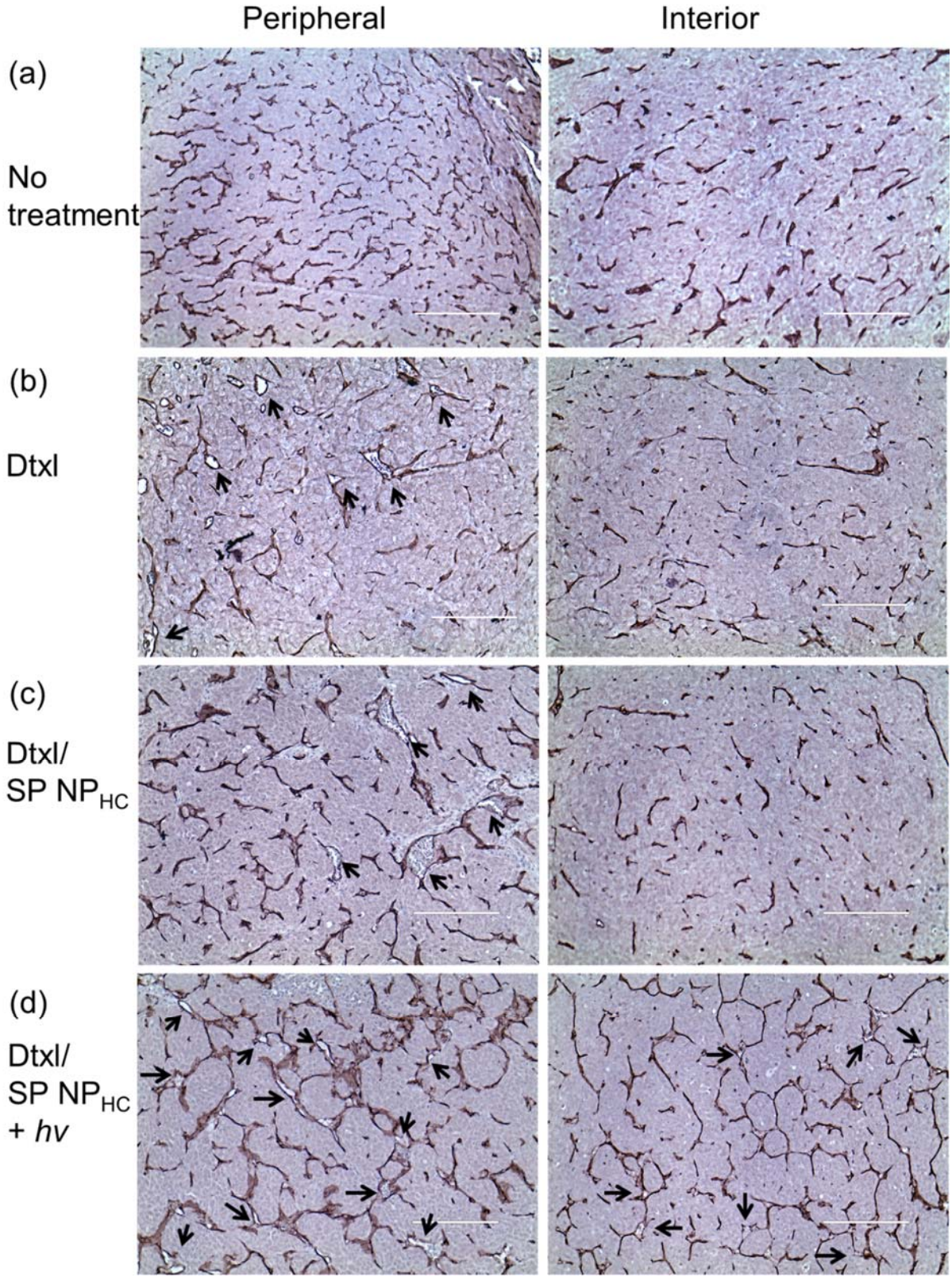
Peripheral
Interior
(a)
No treatment
(b)
Dtxl
(c)
Dtxl/ SP NP$_{HC}$
(d)
Dtxl/ SP NP$_{HC}$ + *hv*

Figure S12. Representative immunohistological images of HT-1080 tumors stained with antibody against CD31 (endothelial marker). (a) no treatment, and 24 hours after i.v. injection with (b) Dtxl, (c) Dtxl/SP NP_{HC}s and (d) same Dtxl/SP NP_{HC}s with irradiation of the tumor site (20s, 1W/cm^2, 30 min post-injection). The Dtxl dose in all formulations was 40 mg/kg. Decompressed vessels with open lumens are indicated by arrows. Left panels: periphery of tumor (<1mm from tumor edge). Right panels: interior of tumor (> 1mm from tumor edge). All vessels are stained by anti-CD31. Scale bar: 200 μm.

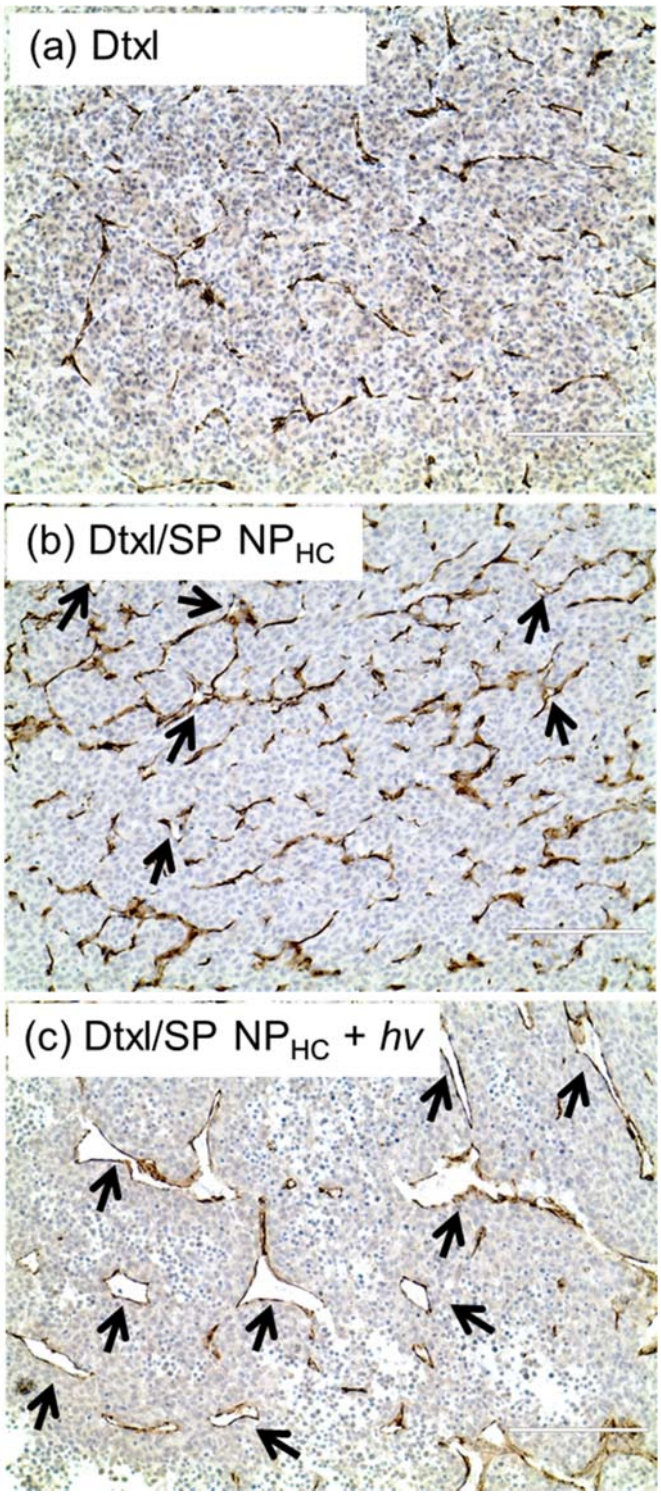

Figure S13. Immunohistological images of subcutaneous HT-1080 tumors stained with anti-CD31 antibodies, 96 h post injection with (a) Dtxl; (b) Dtxl/SP NP_{HC}s and (c) same NP_{HC}s with light triggering on tumor. Dtxl dose in all formulations: 40 mg/kg. Anti-CD31 staining was used to identify blood vessels. Decompressed vessels are indicated by arrows in (b) and (c). Scale bar: 200 μm.

Table S1. Dtxl loadings and size changes upon UV light-triggering* of photo-switchable SP NP_{HCS}

Drug	Theoretical LD %	Actual LD %	LD efficiency %	$Size_{pre}$ (nm)	PD	$Size_{UV}$ (nm)	PD
-	-	-	-	103.5 ± 4.1	0.024	49.2 ± 6.3	0.051
Dtxl	3	2.89 ± 0.05	96.3	84.7 ± 2.9	0.033	47.7 ± 5.8	0.046
Dtxl	5	4.78 ± 0.09	95.6	86.9 ± 4.7	0.060	41.5 ± 6.0	0.072
Dtxl	10	9.41 ± 0.10	94.1	83.3 ± 4.2	0.071	40.8 ± 5.9	0.066
Dtxl	15	12.63 ± 0.31	84.2	93.5 ± 5.9	0.072	48.2 ± 5.4	0.065

* Determined by DLS and HPLC. Abbreviations: LD: loading. PD: polydispersity. $Size_{pre}$: NP_{HCS}' size prior to irradiation. $Size_{UV}$: NP_{HCS}' size after UV irradiation. Data are mean ± SD (N=5).

Table S2. HT-1080 tumor growth inhibition by intravenous treatments (see Figures 3a-b).

Group	Dtxl Dosage (mg/kg)	Tumor Volume Doubling Time (day)	$N_{tr}/N_{ntr}/N_{eu}$	Maximum Body Weight Loss % (day n)	median TTE (Q_{25}, Q_{75})	TTE-TTE_{PBS} (day)	TGD %
PBS	-	2.98	0/0/5	-	7.2 (4.2, 10.3)	-	-
Dtxl	40	**	3/0/2	26.7 (4)	4 (2, 4)	**	-
Dtxl/SP NP_{HC}	40	7.55	0/0/5	2.05 (2)	15.8 (14.7, 17.9)	8.6	119
Dtxl/MC NP_{HC}	40	*	0/0/5	12.1 (4)	53 (31.6, 70)	45.8	636
Dtxl/SP NP_{HC} *+hv*	40	*	0/0/2	10.0 (4)	100 (30.3, 100)	92.8	1289

TTE: time (days) to the end point — time to reaching a tumor volume over 500 mm^3 (tumor diameter ~ 1 cm), when animals are euthanized. N_{tr} is the number of treatment-related deaths. N_{ntr} is the number of non-treatment-related deaths. N_{eu} is the number of mice euthanized because their tumor volumes exceeded 500 mm^3.TTE - TTE_{PBS} is the difference between TTE (days) of each treatment group and that of the PBS group. TGD% (tumor growth delay) = (TTE - TTE_{PBS})/TTE_{PBS}. *The tumor doubling time data were not calculated because the data could not be fit to an exponential growth curve as there was no tumor growth in the first 2 weeks. **: the Dtxl group study was terminated within 4 days due to significant body weight loss (>20%); therefore, and so could not be compared to the TTE in the PBS group. Q_{25}, 25% percentile, Q_{75}, 75% percentile.

Table S3. Plasma pharmacokinetic parameters for Dtxl, Dtxl/SP NP_{HC}, and Dtxl/SP NP_{HC}+*hv* after a single bolus intravenous injection in HT-1080 tumor-bearing nu/nu mice (see Figure 3c).

Group	$t_{1/2\alpha}$ (min)	$t_{1/2\beta}$ (min)	V_d (mL/kg)	AUC (h·mg/mL)	CL (mL/h)
Dtxl	-	14.09	-	0.120	2.090
Dtxl / SP NP_{HC}	42.54	376.12	163.53	0.679	0.368
Dtxl / SP NP_{HC}+*hv*	44.78	212.89	98.19	0.771	0.324

$t_{1/2\alpha}$, plasma distribution half-life; $t_{1/2\beta}$, plasma elimination half-life; V_d, volume of distribution; AUC, area under the concentration—time curve; CL, total body clearance volume.

Supporting information

S1. General Information. Docetaxel (Dtxl) was purchased from LC Laboratories (Woburn, MA) and stored at −20°C prior to use. DSPE-PEG was purchased from Laysan Bio (Arab, AL). Cy5(1) and SP(2) were synthesized according to published procedures. All other chemicals were purchased from Sigma-Aldrich (St Louis, MO) and used as received unless otherwise noted. HPLC analysis was performed on a Hewlett Packard/Agilent series 1100 (Agilent, Santa Clara, CA) equipped with an analytical C18 reverse phase column (Kinetex, 75 × 4.6 mm, 2.6 μ, Phenomenex, Torrance, CA). The UV wavelength for docetaxel analysis was set at 227nm. NMR studies were performed on a Varian 500 system (500 MHz). The sizes and polydispersities of NPs were determined on a ZetaPALS dynamic light-scattering (DLS) detector (15 mW laser, incident beam = 676 nm, Brookhaven Instruments, Holtsville, NY). Fluorescence microscopy was conducted on an Axiovert 200M Zeiss microscope. UV light for produced with a Dymax Bluewave 75 (Torrington, CT).

S2. Preparation of SP NP_{HC}s. DSPE-PEG solution (200 μL, 1 mg/mL in 4 wt% methanol aqueous solution) was freshly prepared in a vial. SP-C9 in acetonitrile or dimethylformamide (DMF, 400 μL, 1mg/mL) was first mixed with cholesterol (0.5 mg/mL, 12 μL) and docetaxel, and carefully pipetted into DSPE-PEG solution. Deionized water (3800 μL) was added and the resulting solution mixture was sonicated in a capped glass vial for 10 minutes using a Branson 2510 bath sonicator (Cleveland, OH) at a frequency of 40 kHz and power of 130W. The resulting NP_{HC}s were collected after ultrafiltration (5 min, 3000 × g, Ultracel membrane with 30,000 Da molecular weight cut-off, Millipore, Billerica, MA), and washed with water to remove organic solvent. The sizes of NP_{HC}s were characterized by DLS.

S3. Determination of Drug (or Dye) Release Kinetics. To determine the release kinetics of SP NP_{HC}s loaded with Dtxl, a PBS suspension of NPs was placed into Slide-A-Lyzer dialysis tubes (300 μL each tube) with a molecular weight cutoff at 3500 Da (Pierce, Rockford, IL). These microtubes were individually dialyzed in 2 L of PBS buffer (1X) at 37 °C. PBS buffer was changed every 24 hours. At scheduled times, the NP solutions from microtubes were collected. DMF (300 μL) was added to dissolve the NPs, and the Dtxl content in each tube was measured by HPLC. That content was serially subtracted from the measured starting quantity of Dtxl to determine release kinetics.

S4. Cytotoxicity of light-triggered Dtxl/SP NP_{HC} NPs. HT-1080 cells were grown in 6-well plates in Minimum Essential Medium (MEM, Invitrogen, Carlsbad, CA), supplemented with 100 units/mL aqueous penicillin G, 100 μg/mL streptomycin, and 10% FBS at concentrations to allow 70% confluence in 24 h (i.e., ~50,000 cells per cm^2). On the day of experiments, cells were washed with prewarmed PBS and incubated with prewarmed phenol-red reduced Opti-MEM media for 30 min before the addition of the Dtxl/SP NP_{HC} (50 μg) NPs loaded with Dtxl (9.4 wt%). The cells were incubated in DMEM medium for 4 h at 37°C, washed with PBS (2× 500 μL per well) and subsequently triggered by UV light for 10s. The cells were further incubated with DMEM medium for 20 h. The cytotoxicity of cells was determined by MTT assay (Sigma-Aldrich, St Louis, MO).

S5. Diffusion of ICG/SP NP_{HC}s in collagen gels. Collagen hydrogels were prepared by mixing the following components on ice, in this order: 8.6 mg/mL rat tail collagen I (200 μL, BD Biosciences, Bedford, MA), 1M sodium hydroxide (207 μL), and 170 mM EDTA (55 μL). The final concentration of collagen I in 462 μL gel solution was 3.72 mg/mL and EDTA was 20 mM. After vortexing, the gel was added to partially fill a microslide capillary tube (Vitrocom, Mountain Lakes, NJ), then incubated for 3 h at 37 °C. 50 μL of Cy5/SP NP_{HC}s (0.1 mg) solution was placed into the capillary tube with a 30 gauge syringe, in contact with the surface of the collagen gel. The tube was sealed and left at 37 °C for 12 h then imaged by using a near infrared laser scanner (LICOR Odyssey, Lincoln, NE). Image analysis was performed by ImageJ. The fluorescence intensity (Cy5 concentration) profile (C) and the distance (x) traveled by the NP_{HC}s with and without irradiation were fitted to the following one-dimensional diffusion model (equation (1))(3-5) to obtain the diffusion coefficient D in the collagen gel:

$$C(x,t) = a \cdot erfc\,(x/(2\sqrt{t \cdot D})) + b \quad (1)$$

where *erfc* is the complementary error function and a, b are the constants for the function. The curve was fitted by Origin 8 software (Northampton, MA).

S6. Animal irradiation timing. For intravenous injection, our PK study (Figure 3c) showed $t_{1/2\alpha}$ (plasma distribution half time) ~40 min, which indicates that ~40-50% particles is already distributed in all tissues 30 min post injection. We hypothesized that the triggered release and size change in particles could change the tumor microenvironment and potentially increase the possibility of intratumoral accumulation for the remaining particles in circulation.

S7. Animals, HT-1080 s.c tumor model and tumor growth inhibition study. HT-1080 cancer cells (American Type Culture Collection, Manassas, VA) were cultured in Minimum Essential Medium supplemented with 100 units/mL aqueous penicillin G, 100 μg/mL streptomycin, and 10% FBS (all from Life Technology, Grand Island, NY). Immuno-deficient nu/nu nude mice were purchased from Charles River Laboratories (Wilmington, MA, USA) and maintained under pathogen-free conditions. Feed and water were available *ad libitum*. The study protocol was reviewed and approved by the MIT Committee on Animal Care. For all *in vivo* studies, 6- to 8-week nude mice (20-25 grams) were implanted with HT-1080 cells by subcutaneous injection in the flank of 1×10^6 cells /0.2 mL in 1:1 (v/v) MEM and matrigel (BD Biosciences, Franklin Lake, NJ). Tumors that reached ~ 50 mm^3 were used for intratumoral injection, and volumes ~ 100 mm^3 for intravenous injection. Intratumoral injection was performed with a syringe pump (Harvard Apparatus, Holliston, MA) at a flow rate of 10 μL/min with total volume of 30 μL. Intravenous injection was administrated via tail-vein injection with total volume of 200 μL. Docetaxel was dissolved in ethanol/Cremophor EL (v/v=1/1) solution for injection. The body weight and tumor size were measured every 2-3 days. Tumor length and width were measure with calipers, and the tumor volume was calculated using the following equation: tumor volume = length × width × width / 2 (6).

Each animal was euthanized when the tumor volume reached a predetermined end point (500 mm^3). The time to the end point (TTE) for each mouse was calculated from the equation TTE=[log (endpoint-b)]/m, where b and m are intercept and slope, respectively, of the line obtained by linear regression of a log-transformed tumor growth data set comprised of the first observation that exceeded the study end volume for each mouse. Animals that did not reach the end point were assigned as a TTE value equal to the last day of the study. Tumor growth delay (TGD) was defined as the increase in the median time to the end point in a treatment group compared with the control group (animals injected with phosphate buffered saline).

S8. Determination of the collagen content of the HT-1080 Tumor Interstitial Matrix. The biochemical analysis of HT-1080 tumor collagen composition was performed on subcutaneous tumors 6-8 mm in diameter. Tumor tissues were surgically excised, cut in three pieces (~50 mg) and rapidly frozen in liquid nitrogen for storage. On the day of experiment, samples were finely dispersed with a homogenizer, solubilized in 1 mL of digest buffer (125 μg/mL papain in 0.1 M sodium phosphate, 5 mM EDTA and 5 mM cysteine, pH=6.0) and incubated at 60 ^oC for 18 hours. After samples returned to room temperature, the hydroxyproline content of collagen fibers in the lysate was assessed by colorimetry, using the Ehrlich solution (Sigma Aldrich, 1.0 M p-dimethylaminobenzaldehyde in 70% isopropanol / 30% perchloric acid) which forms a chromophore with hydroxyproline. The absorption of samples and a hydroxyproline standard solution was measured at 550 nm; the concentration of hydroxyproline in lysate was calculated by fitting to a pre-determined absorption / hydroxyproline standard solution concentration line. Purified collagen type I (BD Pharmingen), in which the hydroxylproline / collagen ratio is reported to be approximately 6.8 (7), was used as reference to estimate the mg of collagen in tumor tissues.

S9. Immunostaining and quantification. For immunohistochemistry, tumors were collected, formalin-fixed and paraffin-embedded. Tissue blocks were cut into 5-10 μm sections for hematoxylin & eosin stain or anti-CD31 stain. To assess vessel density and diameters, tumor sections were stained with the rabbit anti-CD31 antibody (Abcam, MA) using the avidin-biotin peroxidase procedure. Dewaxed sections were rehydrated and heat-mediated antigen-retrieved (pH 6 sodium citrate buffer, 3 min in pressure cooker ~120 ^oC) . The slides were placed in normal rabbit serum or bovine serum albumin for 20 min and then

incubated overnight at 4°C with anti-CD31 diluted 1:50 in normal rabbit serum. The slides were then incubated with goat anti-rabbit biotinylated antibody, followed by peroxidase-conjugated avidin (Abcam, MA). After the diaminobenzidine reaction, the sections were counterstained with hematoxylin. Areas of high vessel density (hot spots) were identified by NIH ImageJ and counted by Image-Pro Plus (MediaCybernetics, Rockville, MD). Vessel diameters were measured as the minimum axis of the best fit-ellipse to the lumen by ImageJ. Vessel counts were expressed as the number of vessels per field (microscopy magnification ×40) .

For fluorescent immunostaining, tumor tissues were excised, snap-frozen, embedded in optimum cutting temperature compound (O.C.T., Sakura Finetek USA, Torrence, CA) and cut into 5-10 μm histological sections. Samples were fixed in cold acetone and blocked for 1 hour at room temperature in PBS buffer containing 1% bovine serum albumin. Samples were incubated with rabbit anti-mouse CD-31 (1:50, Abcam) or rabbit polyclonal anti-ki67 (1:100 Abcam) for 12 h. The corresponding secondary antibodies were added and incubated for 1 h at room temperature: Alexa Fluor 594 goat anti-rat IgG (1:500, Invitrogen) for CD-31 and Alexa Fluor 594 goat anti-rabbit IgG (1:500, Abcam) for ki67. The slides were washed three times with PBS and mounted in Vectashield® Mounting Medium containing DAPI (Vector Laboratories). TUNEL staining (TUNEL apoptosis detection kit with TMR red; Roche) was carried out directly after cold acetone fixing. Imaging were performed with an inverted Zeiss fluorescence microscope model Axiovert 200M (Thornwood, NY). For tumor penetration depth quantification, the extravasation pattern was analyzed by Image-Pro Plus, by drawing ring around vessel walls to generate fluorescence intensity profile. The penetration depth was calculated as the distance to the point where fluorescent intensity was half-maximal (8-10).

S10. Pharmacokinetic study. Mice were injected intravenously with NPs or Dtxl. At predetermined time intervals, <30 μL of blood was collected retro-orbitally in pre-weighed heparinized tubes and centrifuged to obtain the plasma. Cold methanol (300 μL) was added into the plasma to precipitate proteins and extract Dtxl. The mixture was centrifuged at 12,000 rpm for 10 minutes. The concentration of Dtxl in the supernatant was measured by HPLC, taking into consideration that plasma constitutes ~55% of blood volume. The analysis of the results was carried out using Origin 8 software (Northampton, MA) by fitting the concentration-time curve into a two-compartment model according to equation (2).

$$C(t)=ae^{-\alpha t} + be^{-\beta t} \quad (2)$$

Here a, b, α, β are all constants fitted by Origin 8 software (Northampton, MA); α indicates the distribution phase and β the elimination phase in circulation. All other parameters can be calculated based on the equation (2).

S11. Biodistribution study. Mice were sacrificed 24 hours post-injection and organs were collected. ~100 mg of organ tissues were weighed and homogenized in 1 mL CelLytic™ tissue lysis buffer (Sigma-Aldrich) on ice for 1 minutes; and the homogenization was repeated for 5-10 times at 5-min intervals to allow complete decomposition of bulk tissue. Samples were chilled in ice during the 5-min interval. Cold methanol (500 μL) was added to the homogenate; mixtures were vortexed for 2 minutes and then centrifuged at 12,000 rpm for 15 minutes (5415D Microcentrifuge, Eppendorf). To determine the level of Dtxl in each tissue homogenate sample, 500 μL of the supernatant solution was transferred into an HPLC vial and analyzed by HPLC. The data were normalized against the total injected dose per tissue mass (% I.D./g).

S12. Blood chemistry studies. At day 14, mice blood (~1mL) was collected by intracardiac puncture under deep anesthesia with isoflurane at time of sacrifice. Blood was immediately separated into Microvette® capillary blood collection tubes (~0.1 mL, Sarstedt) for CBC/w test (RBC, WBC, HCT, Platelet, RBC indices and manual WBC diffential w/ RBC morphology evaluation), and Microtainer® serum separator tubes (~0.8 mL, BD bioscience) for blood chemistry tests. The tubes were then vortexed and analyzed by the MIT pathology lab.

S13. Lectin perfusion. To address whether the vessels under consideration were actually functional blood vessels, we injected FITC-labeled *lycopersion esculentum* (tomato) lectin (Vector Laboratories) as

a marker of the blood perfusion. The lectin was injected systemically at 10 μL/g of body weight 10 min before fixation.

S14. Statistical Analysis. Animal data are presented as median ± quartiles. Differences between groups were assessed with a Mann-Whitney U test; Kaplan-Meier survival differences were analyzed by the log-rank test. All data analyses were performed using Origin 8 software (Northampton, MA).

References

1. Shmanai VV*, et al.* (2008) A convenient synthesis of cyanine dyes: Reagents for the labeling of biomolecules. *Eur. J. Org. Chem.* (12):2107-2117.
2. Buncel E, Wojtyk JTC, & Kazmaier PM (2001) Modulation of the spiropyran-merocyanine reversion via metal-ion selective complexation: Trapping of the "Transient" cis-merocyanine. *Chem. Mater.* 13(8):2547-2551.
3. Clauss MA & Jain RK (1990) Interstitial Transport of Rabbit and Sheep Antibodies in Normal and Neoplastic Tissues. *Cancer Res.* 50(12):3487-3492.
4. Ramanujan S*, et al.* (2002) Diffusion and convection in collagen gels: Implications for transport in the tumor interstitium. *Biophys. J.* 83(3):1650-1660.
5. Wong C*, et al.* (2011) Multistage nanoparticle delivery system for deep penetration into tumor tissue. *Proc. Natl. Acad. Sci. U. S. A.* 108(6):2426-2431.
6. Euhus DM, Hudd C, Laregina M, & Johnson FE (1986) TUMOR MEASUREMENT IN THE NUDE-MOUSE. *J. Surg. Oncol.* 31(4):229-234.
7. Netti PA, Berk DA, Swartz MA, Grodzinsky AJ, & Jain RK (2000) Role of extracellular matrix assembly in interstitial transport in solid tumors. *Cancer Res.* 60(9):2497-2503.
8. Tong RT*, et al.* (2004) Vascular Normalization by Vascular Endothelial Growth Factor Receptor 2 Blockade Induces a Pressure Gradient Across the Vasculature and Improves Drug Penetration in Tumors. *Cancer Res.* 64(11):3731-3736.
9. Kyle AH, Huxham LA, Yeoman DM, & Minchinton AI (2007) Limited Tissue Penetration of Taxanes: A Mechanism for Resistance in Solid Tumors. *Clin. Cancer Res.* 13(9):2804-2810.
10. Liu J*, et al.* (2012) TGF-β blockade improves the distribution and efficacy of therapeutics in breast carcinoma by normalizing the tumor stroma. *Proceedings of the National Academy of Sciences* 109(41):16618-16623.